Supporting Information for

Effects of Crystalline Perylenediimide Acceptor Morphology on Optoelectronic Properties and Device Performance

Patrick E. Hartnett[1], Eric A. Margulies[1], H.S.S. Ramakrishna Matte[1,2], Mark C. Hersam[1,2], Tobin J. Marks[1,2]*, and Michael R. Wasielewski[1]*

[1] Department of Chemistry and the Argonne-Northwestern Solar Energy Research Center, Northwestern University, 2145 Sheridan Road, Evanston, Illinois 60208, USA

[2] Department of Materials Science and Engineering and the Materials Research Center, Northwestern University, 2145 Sheridan Road, Evanston, Illinois, 60208, USA

Synthesis

Phenylboronic acid neopentylglycol ester was synthesized according to reported literature procedures.(REF) Pinacolone and mesitylene, were purchased from Sigma-Aldrich (St. Louis, MO) and distilled over CaH prior to use. RuH2(CO)(PPh3)3 was purchased from TCI (Portland, Oregon). Column chromatography was performed using silica gel from Sorbent Technologies (Atlanta, GA). All solvents were spectrophotometric grade unless otherwise noted. ^{1}H nuclear magnetic resonance spectra were obtained on a Bruker Avance III 500MHz spectrometer. Matrix-assisted laser-desorption-ionization time-of-flight (MALDI-TOF) mass spectra were obtained using a Bruker Daltonics Autoflex III Smartbeam MALDI mass spectrometer in negative ionization mode without matrix.

General Synthesis of Headland Phenyl PDIs

NN'-bis-alkyl-3,4,9,10-perylenediimide (0.162 mmol) and phenylboronic acid neopentylglycol ester (217 mg, 1.14 mmol) were mixed with $RuH_2(CO)(PPh_3)_3$ (30 mg, 0.032 mmol) in a 5 mL conical vial and sealed, evacuated, and backfilled with nitrogen. Pinacolone (1 mL) and mesitylene (1 mL) were distilled, degassed, and added to the vial and the mixture was heated to 140°C and stirred for 24 hours. The crude product was precipitated with methanol, redissolved in dichloromethane, and purified by column chromatography (3:1 DCM:Hexanes). The first red band was collected in each case, the solvent was removed, and the resulting solid was dissolved in a minimal amount of dichloromethane and precipitated from methanol to give the product.

Synthesis of N,N-bis(3,7-dimethyloctyl)-2,5,8,11-tetraphenyl-PDI (3,7-DMO). The reaction was conducted according to the general procedure using 110 mg of starting PDI and the product was collected as a bright orange solid (118 mg, 74%). ^{1}H NMR (500 MHz, Chloroform-*d*) δ 8.38

(s, 4H), 7.59 – 7.47 (m, 12H), 7.47 – 7.41 (m, 8H), 3.99 (m, 4H), 1.62 – 0.97 (m, 18H), 0.86 (d, *J* = 6.3 Hz, 6H), 0.83 (d, *J* = 6.7, 12H). ^{13}C NMR (126 MHz, Chloroform-*d*) δ 162.59, 148.43, 142.58, 132.86, 131.34, 128.52, 127.92, 127.85, 125.65, 120.95, 39.36, 37.29, 35.14, 31.42, 28.08, 24.78, 22.83, 22.75, 19.60. MALDI-TOF (*m/z*) $[M]^-$ = 974.574 (Calcd for $C_{68}H_{66}N_2O_4$: 974.502)

Synthesis of N,N-bis(2-ethylhexyl)-2,5,8,11-tetraphenyl-PDI (2-EH). The reaction was conducted according to the general procedure using 100 mg of starting PDI and the product was collected as a dark red solid (135 mg, 90%). ^{1}H NMR (500 MHz, Chloroform-*d*) δ 8.40 (s, 4H), 7.58 – 7.46 (m, 12H), 7.46 – 7.40 (m, 8H), 3.94 (d, *J* = 7.6 Hz, 4H), 1.85 (m, 2H), 1.35 – 1.11 (m, 16H), 0.85 (t, *J* = 6.9 Hz, 6H), 0.83 (t, *J* = 7.6 Hz, 6H). ^{13}C NMR (126 MHz, Chloroform-*d*) δ 163.09, 148.39, 142.50, 132.88, 131.33, 128.53, 127.99, 127.94, 127.76, 125.61, 121.06, 44.27, 37.36, 30.49, 28.62, 23.74, 23.35, 14.24, 10.66. MALDI-TOF (*m/z*) $[M]^-$ = 918.408 (Calcd for $C_{64}H_{58}N_2O_4$: 918.440)

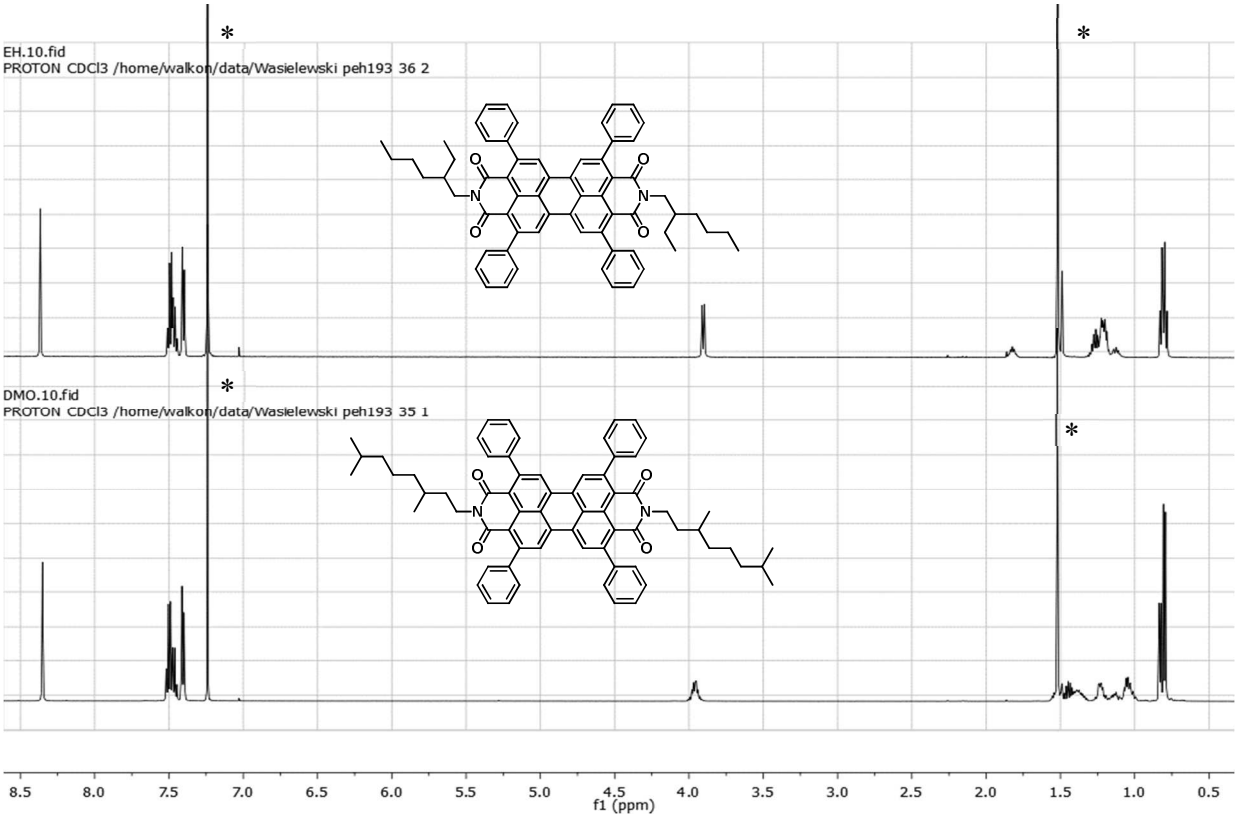

^{1}H NMR Spectra of 2-EH and 3,7-DMO

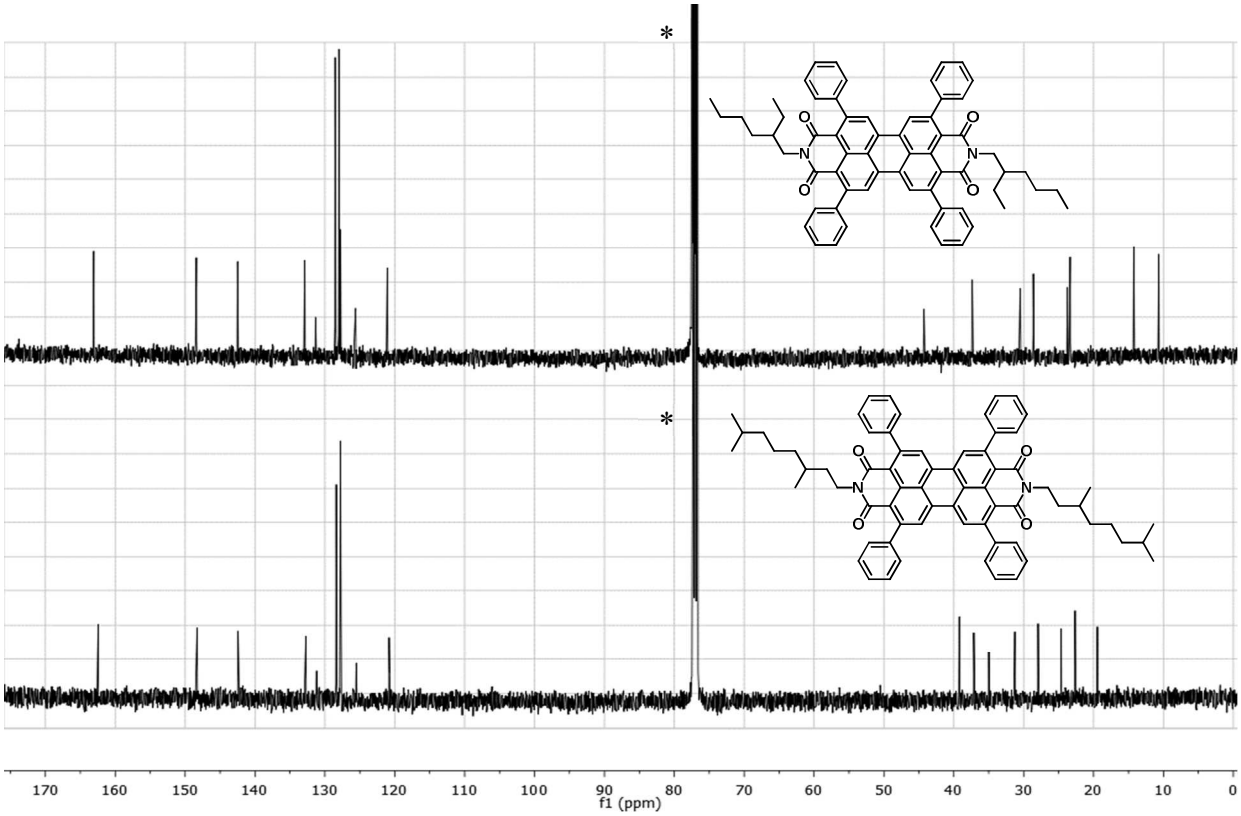

^{13}C NMR Spectra of 2-EH and 3,7-DMO

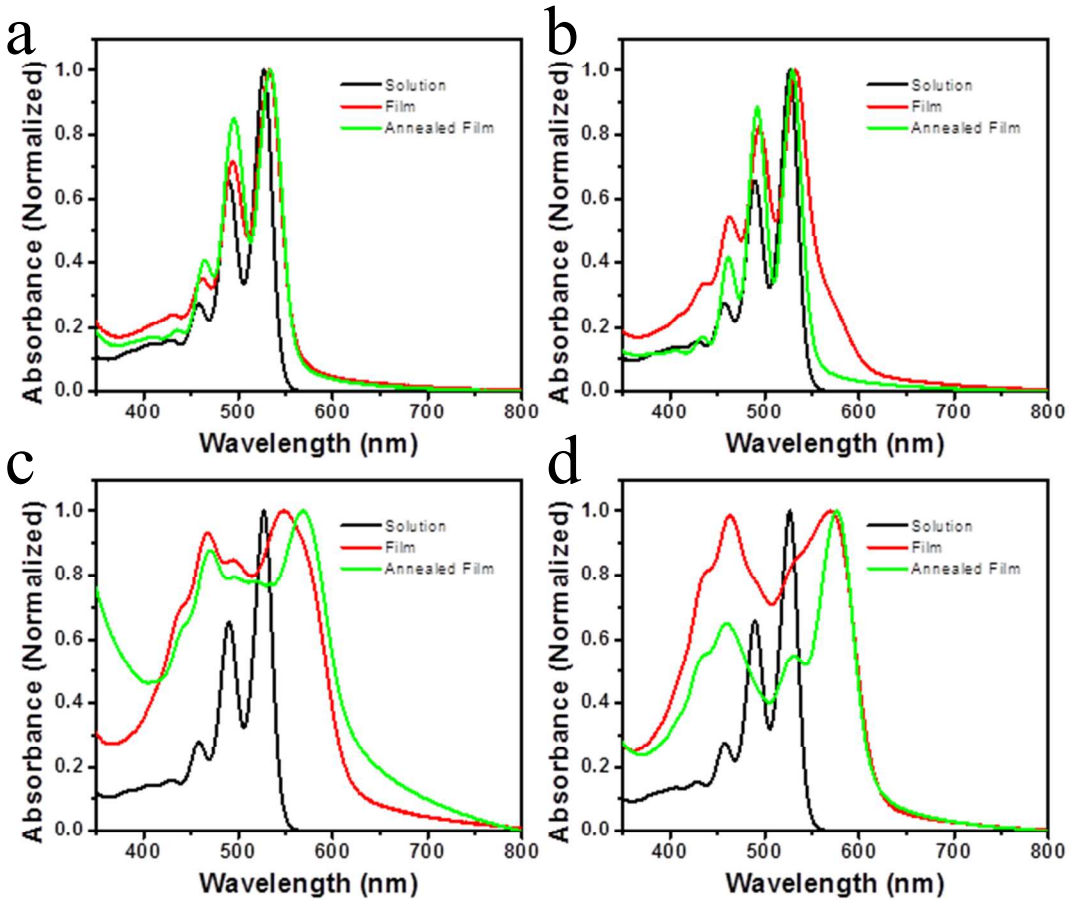

Figure S1: Solution and thin film absorption spectra of **3-pentyl** (a), **3,7-DMO** (b), **2-EH** (c), and **n-octyl** (d). Spectra of pristine thin films (red) and films which were solvent vapor annealed in CH_2Cl_2 for 1 hour (green) are shown.

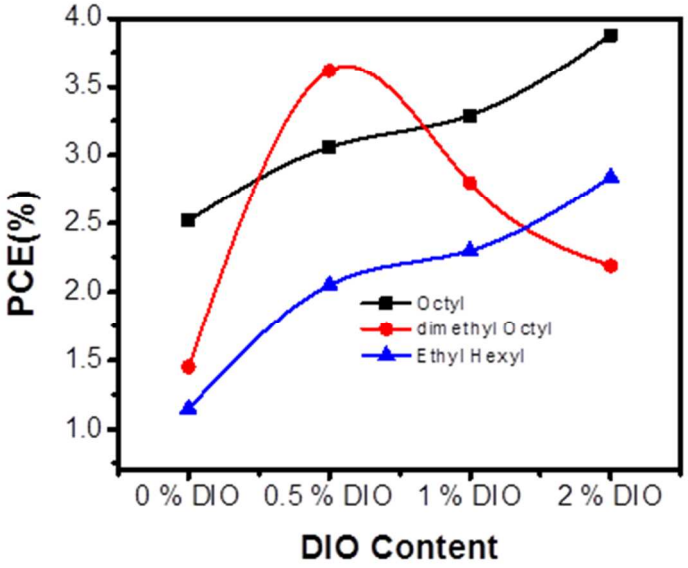

Acceptor	0%	0.5%	1%	2%	2.5%	3%
n-octyl	2.52 (2.38)	3.06 (2.93)	3.29 (3.19)	**3.88** (3.60)	3.18 (2.95)	3.01 (2.86)
3,7-dimethyloctyl	1.45 (1.31)	**3.62** (3.50)	2.82 (2.64)	2.19 (1.97)		
2-ethylhexyl	1.15 (1.08)	2.05 (1.96)	2.30 (2.20)	**2.84** (2.58)	2.52 (2.44)	2.38 (2.27)

Figure S2: OPV device efficiencies of **3-pentyl**, **3,7-DMO**, **2-EH**, and **n-octyl** as a function of DIO concentration. **3-pentyl** is not included because it was processed from chlorobenzene rather than chloroform and its efficiency was not improved by DIO. The average performance over four devices is shown in parentheses.

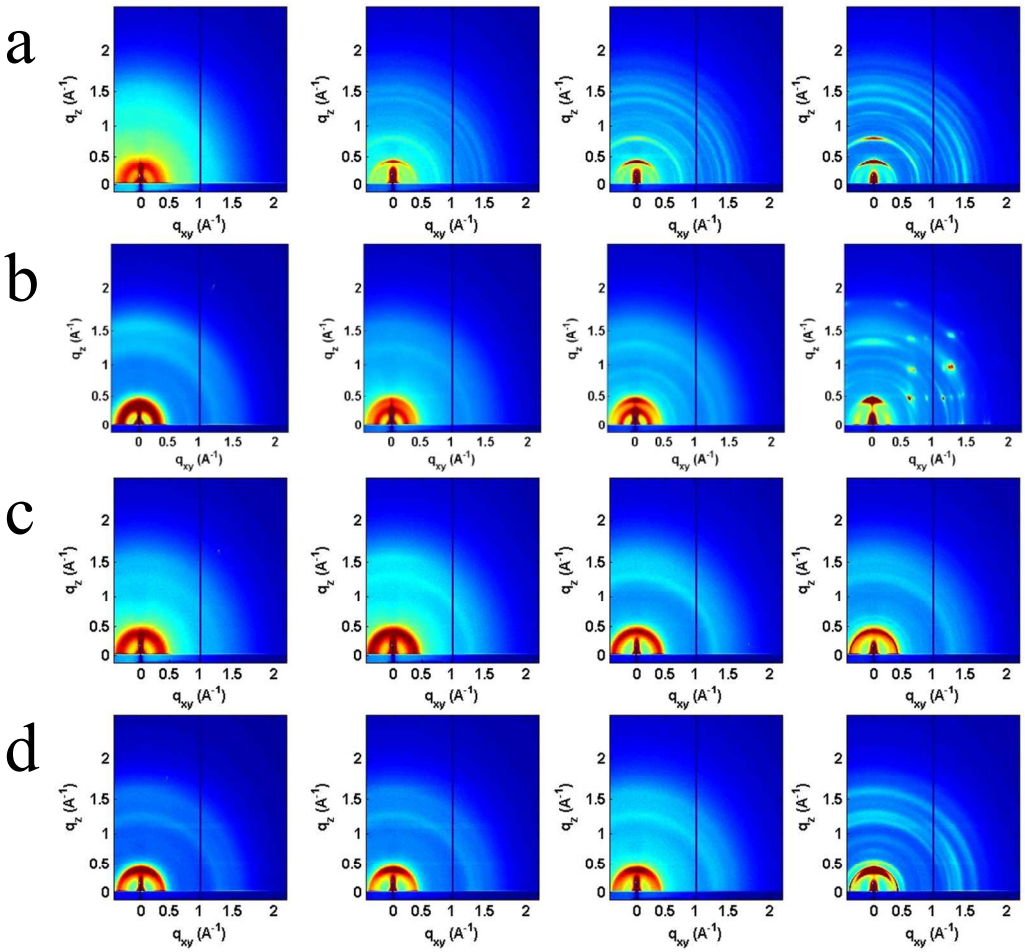

Figure S3: GIWAXS scattering images of of **3-pentyl** (a), **3,7-DMO** (b), **2-EH** (c), and **n-octyl** (d) blend films cast from solutions with 0%, 0.5%, 1%, and 2% DIO (from left to right).

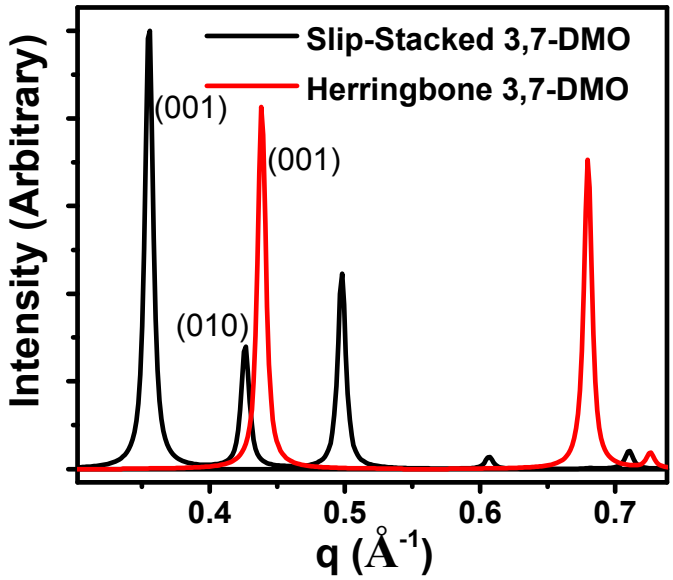

Figure S4: Simulated powder diffraction patterns obtained using the slip-stacked and the herringboned polymorphs of **3,7-DMO**.

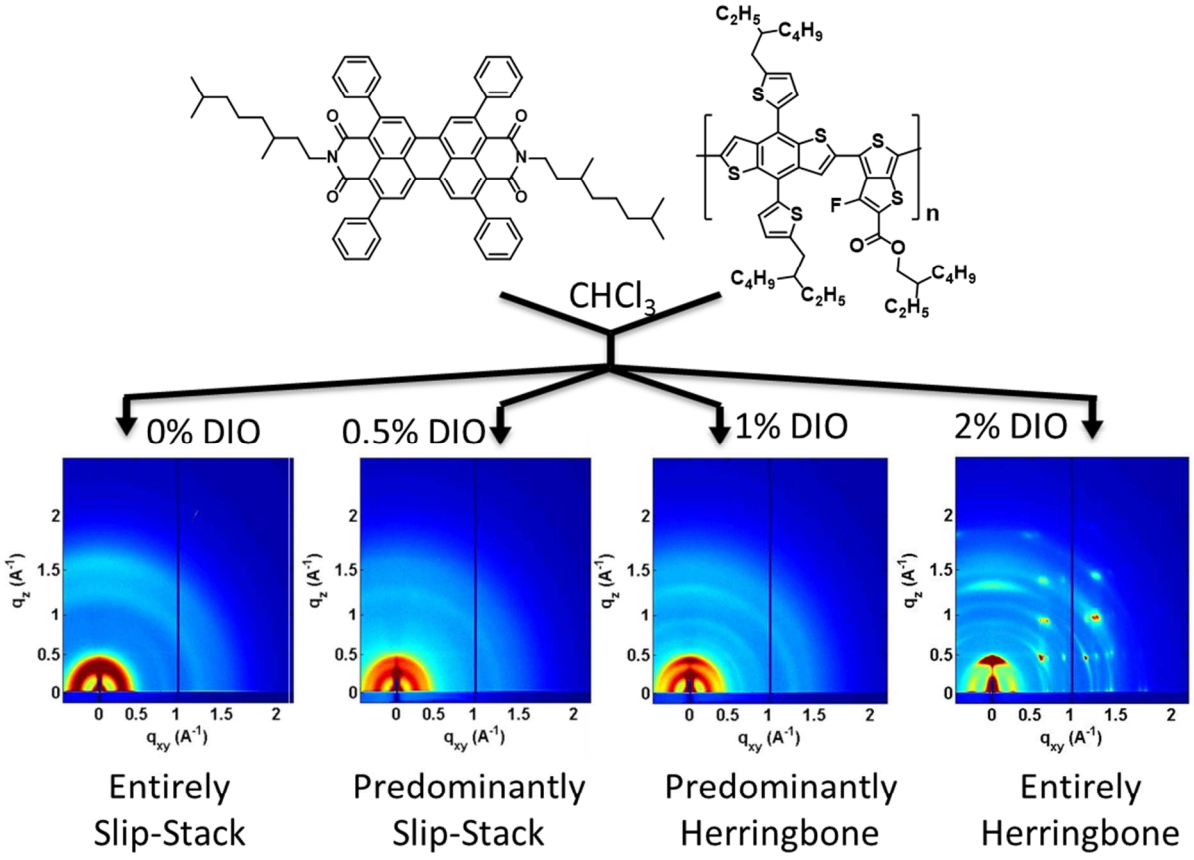

Scheme S1: Summary of morphologies produced under various processing conditions.

Table S1: Scherrer grain size analysis of **3,7-DMO** blend films.

Herringbone (0,0,1)			
Film	**d-Spacing (Å)**	**FWHM**	**D_{hkl} (nm)**
0%	16.6	0.199	2.73
0.50%	14.6	0.134	4.07
1%	14.2	0.094	5.82
2%	14.2	0.067	8.36

Slip-Stacked (0,0,1)			
Film	**d-Spacing (Å)**	**FWHM**	**D_{hkl} (nm)**
0%	16.2	0.136	4.02
0.50%	15.5	0.145	3.77
1%	15.9	0.155	3.52

Polymer Lamellar			
Film	**d-Spacing (Å)**	**FWHM**	**D_{hkl} (nm)**
0%	21.5	0.111	4.92
0.50%	24.2	0.116	4.70
1%	25.1	0.095	5.75
2%	23.1	0.094	5.81

Table S2: PL Quenching of PDI:**PBDTT-FTTE** films.

DIO Content	0 %	0.5 %	1 %	2%
n-octyl	>99%	99%	97%	78%
2-EH	>99%	>99%	97%	93%
3,7-DMO	>99%	98%	97%	77%
3-pentyl	97%	65%	57%	20%

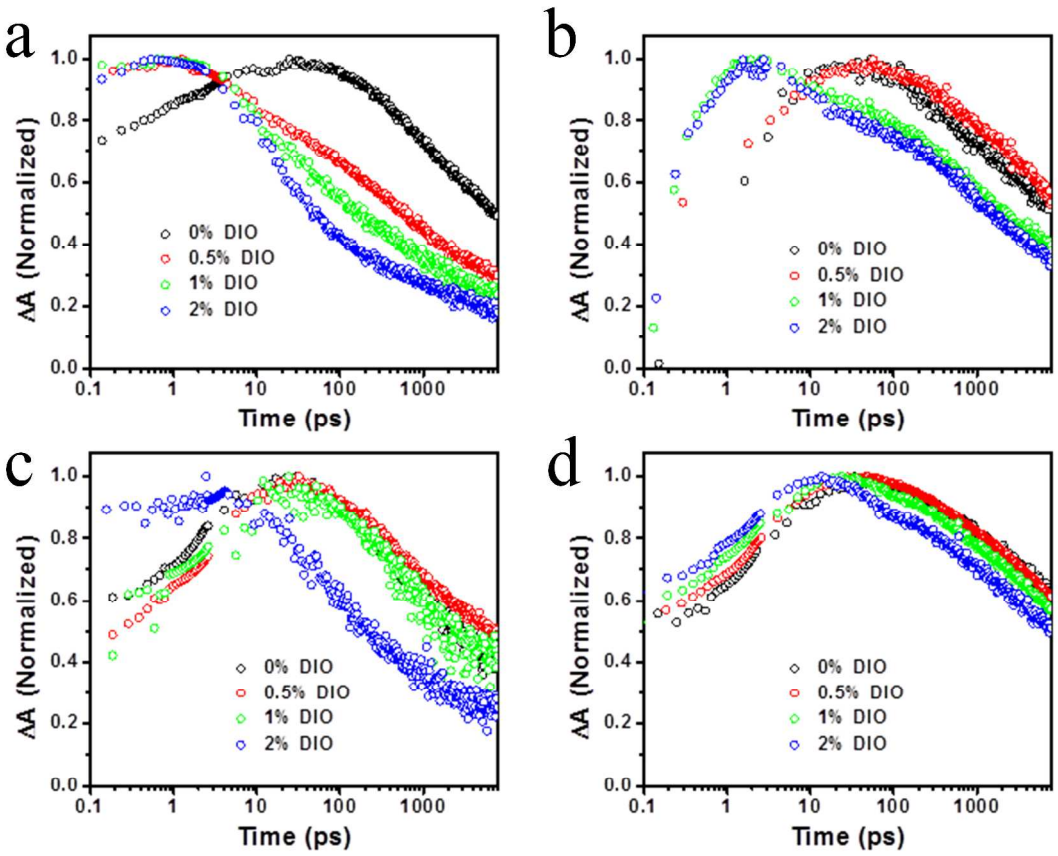

Figure S5: fsTA kinetics of the PDI anion integrated from 770 nm to 800 nm for blend films of **3-pentyl** (a), **3,7-DMO** (b), **2-EH** (c), and **n-octyl** (d).

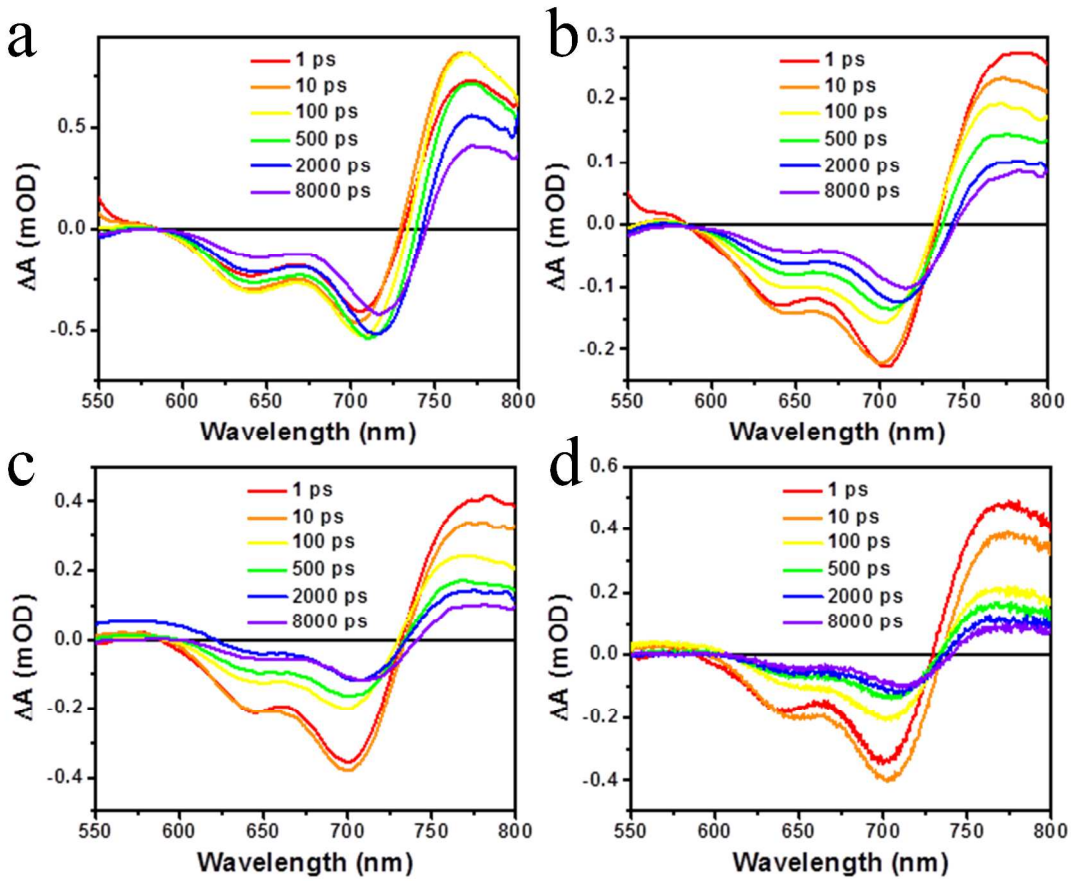

Figure S6: fsTA spectra of blend films of **3-pentyl** cast from solutions containing 0% (a), 0.5% (b), 1% (c), and 2% (d) DIO.

Table S3: fsTA kinetic fits of blend films of **3-pentyl**. The relative magnitude of each component is given in parenthesis. All components correspond to charge recombination unless otherwise stated. Events faster than 0.5 ps are not shown.

0% DIO	0.5% DIO	1% DIO	2% DIO
2.9 ± 0.1 ps (rise)	15.6 ± 0.8 ps (27%)	18.9 ± 0.8 ps (40%)	19.2 ± 0.6 ps (52%)
700 ± 20 ps (31%)	440 ± 20 ps (30%)	370 ± 20 ps (26%)	270 ± 20 ps (20%)
>>10 ns (69%)	>>10 ns (43%)	>>10 ns (34%)	>>10 ns (28%)

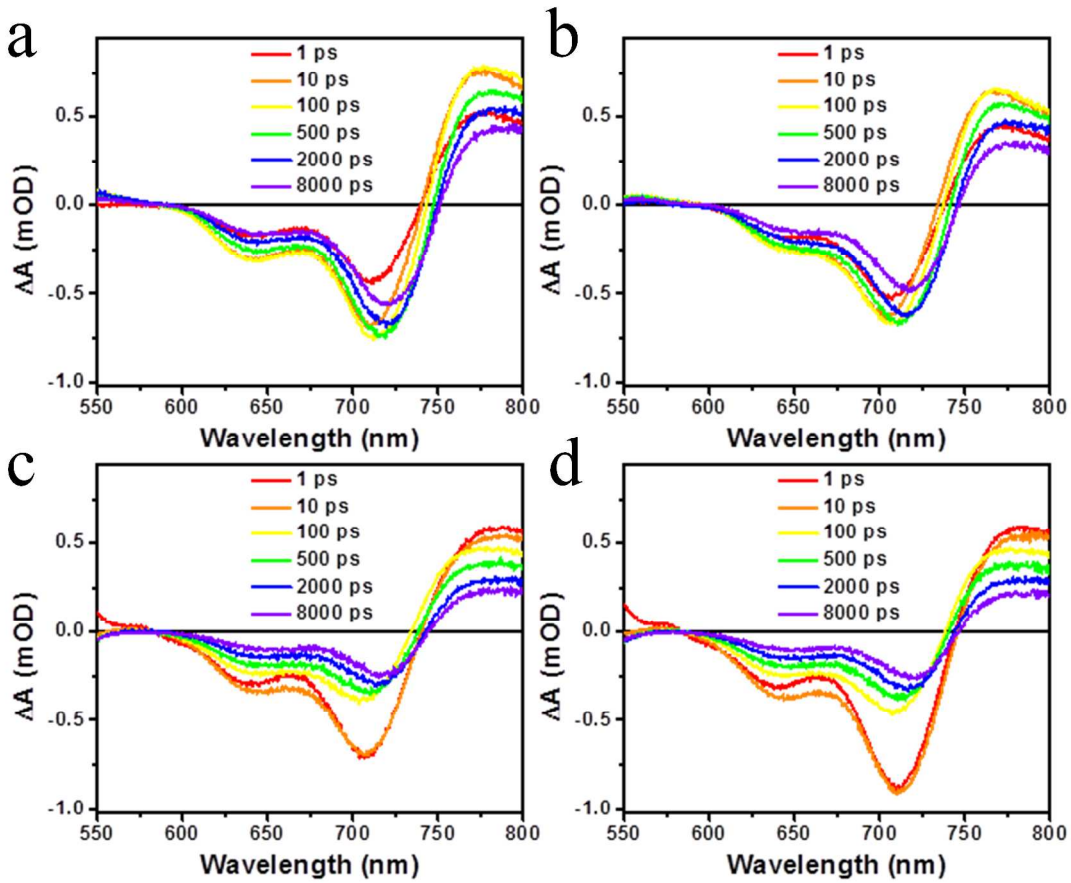

Figure S7: fsTA spectra of blend films of **3,7-DMO** cast from solutions containing 0% (a), 0.5% (b), 1% (c), and 2% (d) DIO.

Table S4: fsTA kinetic fits of blend films of **3,7-DMO**. The relative magnitude of each component is given in parenthesis. All components correspond to charge recombination unless otherwise stated. Events faster than 0.5 ps are not shown.

0% DIO	0.5% DIO	1% DIO	2% DIO
2.0 ± 0.1 ps (rise)	6.5 ± 0.4 ps (rise)	15 ± 1 ps (17%)	18 ± 1 ps (20%)
570 ± 30 ps (29%)	640 ± 30 ps (22%)	600 ± 20 ps (30%)	660 ± 30 ps (28%)
>>10 ns (71%)	>>10 ns (78%)	>>10 ns (53%)	>>10 ns (52%)

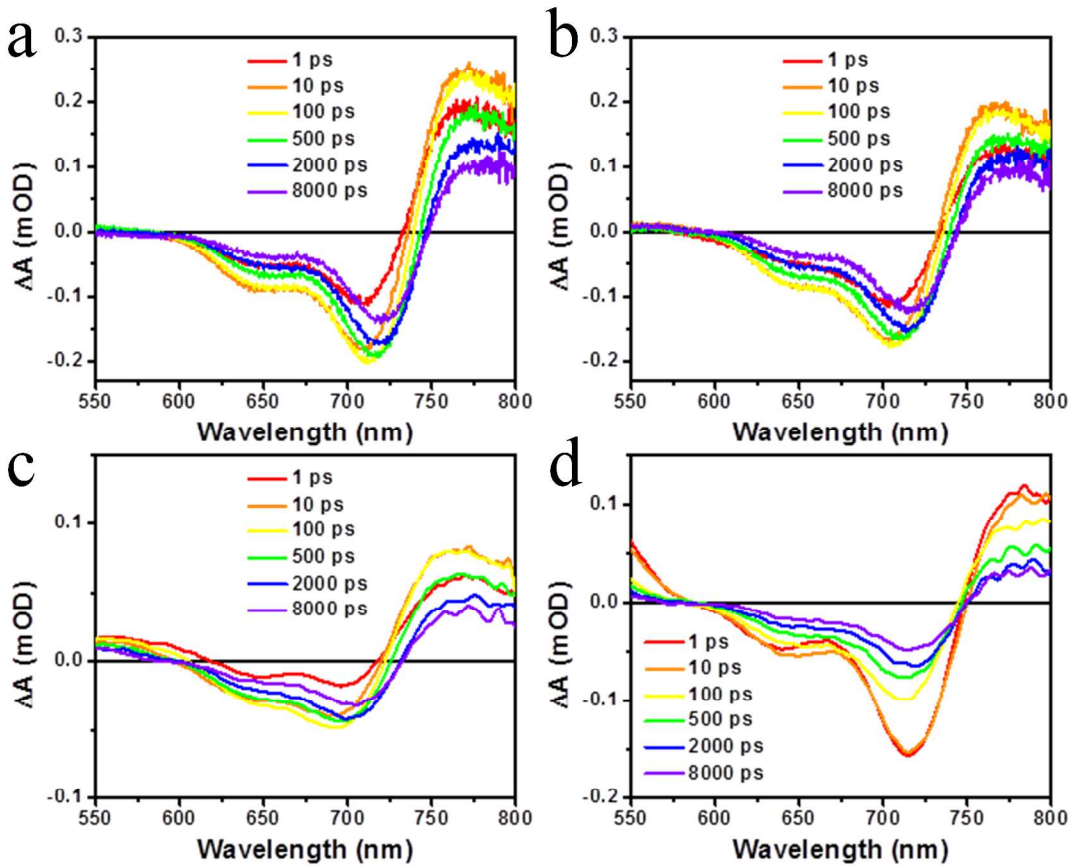

Figure S8: fsTA spectra of blend films of **2-EH** cast from solutions containing 0% (a), 0.5% (b), 1% (c), and 2% (d) DIO.

Table S5: fsTA kinetic fits of blend films of **2-EH**. The relative magnitude of each component is given in parenthesis. All components correspond to charge recombination unless otherwise stated. Events faster than 0.5 ps are not shown.

0% DIO	0.5% DIO	1% DIO	2% DIO
2.7 ± 0.2 ps (rise)	3.9 ± 0.1 ps (rise)	4.3 ± 0.6 ps (rise)	56 ± 4 ps (41%)
460 ± 20 ps (39%)	480 ± 10 ps (34%)	610 ± 40 ps (47%)	680 ± 80 ps (28%)
>>10 ns (61%)	>>10 ns (66%)	>>10 ns (53%)	>>10 ns (31%)

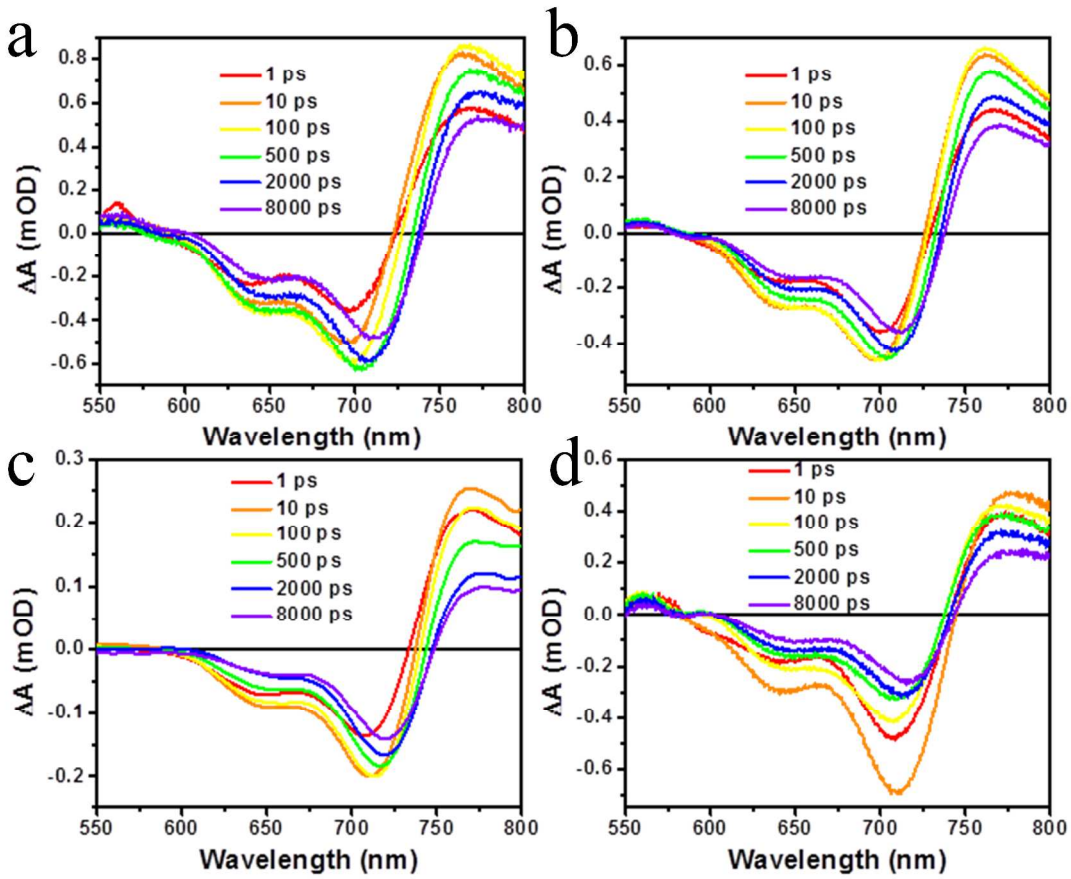

Figure S9: fsTA spectra of blend films of **n-octyl** cast from solutions containing 0% (a), 0.5% (b), 1% (c), and 2% (d) DIO.

Table S6: fsTA kinetic fits of blend films of **n-octyl**. The relative magnitude of each component is given in parenthesis. All components correspond to charge recombination unless otherwise stated. Events faster than 0.5 ps are not shown.

0% DIO	0.5% DIO	1% DIO	2% DIO
3.9 ± 0.2 ps (rise)	3.6 ± 0.1 ps (rise)	2.6 ± 0.8 ps (rise)	2.5 ± 0.1 ps (rise)
630 ± 30 ps (20%)	660 ± 20 ps (20%)	520 ± 20 ps (22%)	56 ± 5 ps (14%) 840 ± 60 ps (20%)
>>10 ns (80%)	>>10 ns (80%)	>>10 ns (78%)	>>10 ns (66%)

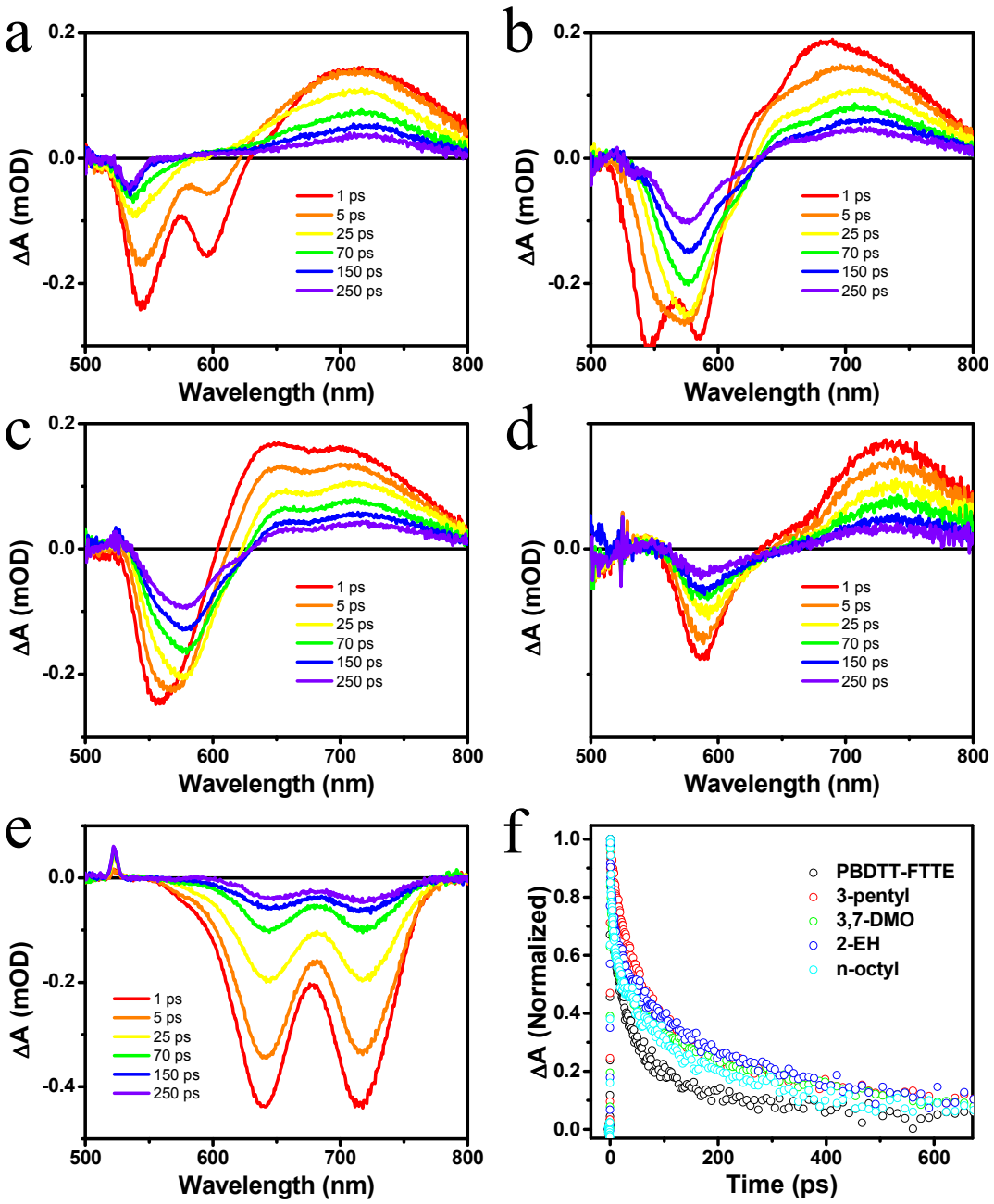

Figure S10: fsTA spectra of pristine films of **3-pentyl** (a), **3,7-DMO** (b), **2-EH** (c), **n-octyl** (d), and **PBDTT-FTTE** (e) and their decay kinetics (f).